

# On the Intra- and Intermolecular Bonding in Polyiodides

Lars Kloo,<sup>\*[a]</sup> Jan Rosdahl,<sup>[a]</sup> and Per H. Svensson<sup>[a]</sup>

**Keywords:** Iodine / Polyhalides / Bond theory

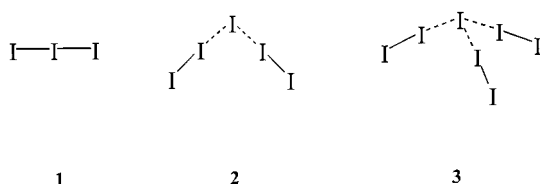
The nature of intra- and intermolecular interactions of polyiodides has been investigated by means of quantum chemical methods and structural statistical data. In the region of "secondary bonds" the interaction is adequately described in terms of covalent bonding accompanied by dispersion. At

greater distances the interaction is dominated by ion-quadrupole interactions between ionic and neutral iodine building blocks of the polyiodide structures.

(© Wiley-VCH Verlag GmbH, 69451 Weinheim, Germany, 2002)

## Introduction

Polyiodides have been extensively studied in the solid and liquid state and are characterized by a strong tendency to concatenation.<sup>[1]</sup> The solid structures may contain small, discrete polyiodides or large, extended anionic networks of interconnected units. Typically, polyiodides are described according to the stoichiometry of the discrete anions or the repeating units of the extended structures, such as triiodides **1**, pentaiodides **2**, heptaiodides **3** etc. Today, repeating units in complex networks have been claimed to contain up to almost 30 iodine atoms, for instance  $I_{29}^-$  in  $(Fc)_3I_{29}$  and  $I_{26}^{3-}$  in  $(Me_3S)_3I_{26}$ .<sup>[2,3]</sup> Almost all these structures can be described as consisting of only three fundamental building blocks:  $I^-$ ,  $I_2$  and  $I_3^-$ .



In this context it is also worth noting that the triiodides occupy a special position in the sense that they typically contain discrete  $I_3^-$  ions with intermolecular I–I contacts near the van der Waals (vdW) distances, forming linear, zig-zag or T-shaped packing patterns. Higher polyiodides can be regarded as constructed from the ions  $I^-$  or  $I_3^-$ , solvated by the neutral solvent molecules  $I_2$ , often into low-dimensional extended networks.

Depending on the extent of intermolecular bonding,  $I_2$  displays I–I bond lengths between 2.69 and 2.80 Å. The triiodide ion is either centrosymmetric with an I–I bond length of about 2.91 Å or belongs to an asymmetric config-

uration with I–I distances between 2.85 and 3.00 Å. Thus, the intramolecular bond-length range for the fundamental building blocks can be defined as 2.69–3.00 Å. The sum of vdW radii for iodine is 4.3 Å and the  $I_2$ – $I_2$  vdW distance is normally set to 3.9–4.0 Å. With this in mind it is interesting to note the large number of intermolecular I–I contacts in the range between 3 and 4 Å. This was made clear by a structural statistical study of pentaiodides by Bittner.<sup>[4]</sup> I–I contacts in the intermediate range between typical intramolecular and vdW distances are normally referred to as "secondary bonds".

The assignment of an I–I contact as a secondary bond seems purely pragmatic. An arbitrary cut-off set to around 3.5 Å often allows a complicated network structure to be described in simpler terms (interconnected iodine molecules, pentaiodides etc.). However, polyiodide chemistry seems to have been focused on the search for larger and larger repeating units (i.e. higher  $I_2$  contents) in recent years, and one can observe a progressive increase in the assigned distance cut-off. Is the secondary bond a completely artificial concept? Which type of interaction predominates at the typical intermolecular I–I distances between 3 and 4 Å? These questions were the motivation for this study.

For instance, pentaiodides ( $I_5^-$ ) are found in three different forms irrespectively of whether they are discrete or part of an extended network: V-shaped  $[(I^-) \cdot 2I_2]$ , L-shaped  $[(I_3^-) \cdot I_2]$  and linear  $[(I^-) \cdot 2I_2]$ . The bonding in these pentaiodides can be described in two principally different ways, in terms of either covalent interactions between mainly valence 5p orbitals or of closed-shell interactions (vdW interactions, charge-transfer interaction or dative bonds) between the building blocks.

The present study relies on statistical data for two archetypal structural fragments in polyiodide chemistry, employing the CSD database, and quantum chemical calculations providing potential energy surfaces (PES), bond order surfaces (BOS) and electron density maps of the same or similar fragments. The PES values obtained for

<sup>[a]</sup> Department of Inorganic Chemistry, Royal Institute of Technology, 10044 Stockholm, Sweden

Hartree–Fock (HF) and correlated levels are used to study the influence of correlation. The difference in energy between HF and correlated methods is axiomatically regarded as a measure of the correlation energy, thus providing information about the dispersion interaction. As pointed out in recent reviews, the interpretation of the PES is far from straightforward.<sup>[5,6]</sup> Although the explicit inclusion of the dynamic electron correlation provides insight into the intermolecular dispersion interaction, it also affects the intramolecular interactions. Therefore, difference PES values contain both intra- and intermolecular effects of correlation. The BOS values used in this work are based on a natural bond population analysis (NPA), although the very same information can be extracted from other types of population analyses, including the democratic method of Mulliken.<sup>[7]</sup>

## Statistics

Figure 1 shows the histogram of the configuration in **4**. The histogram thus represents the “view” from an  $I_2$  molecule with respect to both intra- and intermolecular contacts to another iodine atom. This representation is focused on “ $I_3^-$ ” units in polyiodide structures and consequently is heavily dominated by the intramolecular contacts from 2.7–3.0 Å; the polyiodide structures are mainly triiodides (vide infra). The distribution of I–I contacts is largely uniform over the entire region of “secondary bonds”, i.e. between 3 and 4 Å, whereas an increase is observed at distances greater than 4 Å. The latter effect can probably be attributed to purely statistical/sterical reasons, allowing more neighbours at greater distances. Ideally, an initial parabolic increase would be expected.

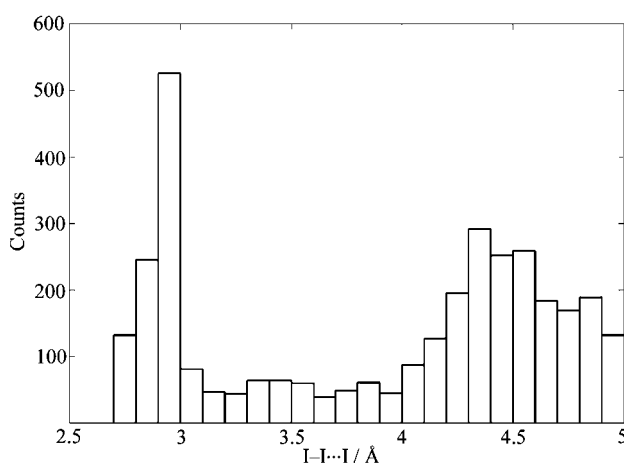


Figure 1. Histogram of the I–I distances from an  $I_2$  fragment

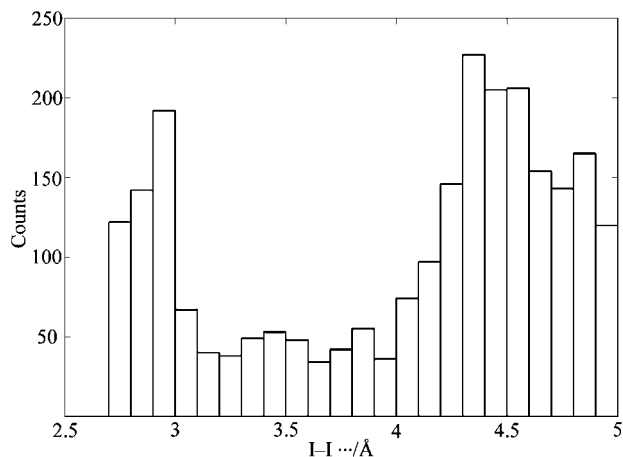
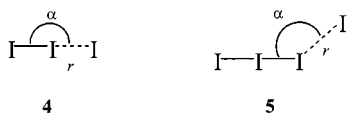


Figure 2. Histogram of the I–I distances from an  $I_3$  fragment

Figure 2 shows the corresponding histogram for configuration **5**. Here, the diagram is completely dominated by intermolecular contacts from the “view” of a triiodide unit. Unfortunately, in the database there are quite a number of structures, in which the intramolecular I–I contacts have not been properly defined. As a result, these will also appear at short distances in this figure, making the overall distribution of I–I contacts very similar to that in Figure 1. Again, a very uniform distribution is observed between 3 and 4 Å.

## The Triiodide System

The PES for  $I_3^-$  at the HF level is shown in Figure 3, corresponding to the configuration in **6**. Here, the distance  $r_1$  and angle  $\alpha$  are changed and the distance  $r_2$  optimized at each point of the PES. It is clear that the preferred structure is centrosymmetrical ( $D_{ih}$ ) with an I–I distance just below 3.0 Å. The intramolecular bonding in trihalide systems was extensively studied and the present results are in good agreement with previous work.<sup>[1,8]</sup> In order to estimate the influence of dynamic correlation, calculations at the MP2 and CCSD levels were also performed. The difference PES at MP2 level is given in Figure 4. Correlation at both levels gives an overall stabilization of the triiodide structure. A minimum valley (corresponding to a maximum in the

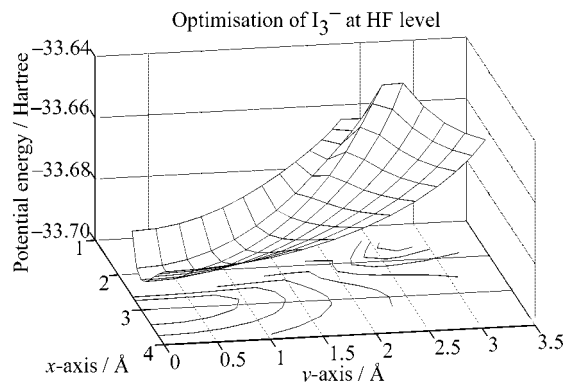


Figure 3. PES at HF level for the  $I_3^-$  ion

correlation stabilization) is observed near the optimum I–I distance (2.965, 2.943 and 2.964 Å for the HF, MP2 and CCSD levels, respectively). Remarkably enough, a minimum in the correlation energy seems to exist at a conformation corresponding to  $D_{3h}$  symmetry. However, this geometry is Jahn–Teller-unstable and not attainable by single-configuration methods. Nevertheless, this permits the conclusion that no obvious extra stabilization results from correlation at distances greater than the equilibrium intramolecular distance in  $I_3^-$ .

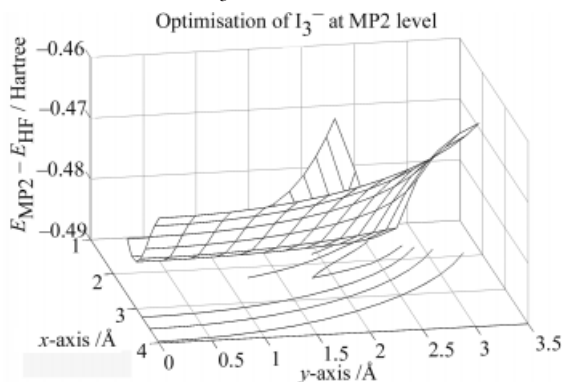
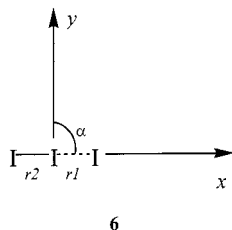


Figure 4. Difference PES between HF and MP2



A plot of the NLMO/NPA BOS at the HF level is given in Figure 5. As expected, the bond order is close to 0.5 at the equilibrium distance and then progressively decreases as the I–I distance is increased. It is also notable that the decrease is less steep for the linear conformation, thus reflecting the behaviour of the corresponding PES. The BOS at the MP2 level is very similar, and the bond order at 4 Å is 0.046 and 0.087 at the HF and MP2 levels, respectively. A naive interpretation of these data suggests the postulation

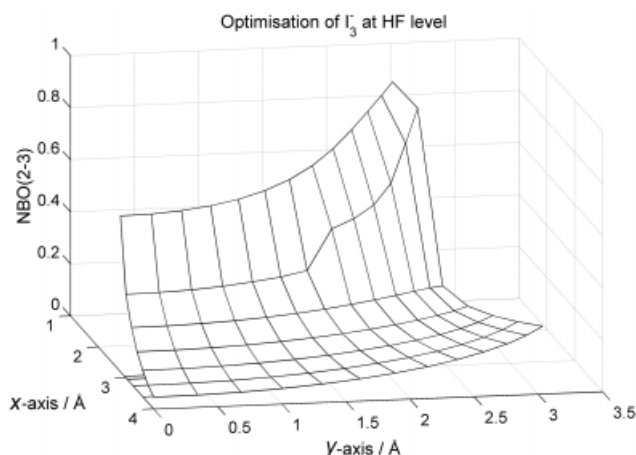


Figure 5. NLMO/NPA BOS for the  $I_3^-$  ion at HF level

of a weak covalent interaction between the  $I_2$  and  $I^-$  fragments extending to the region of the so-called “secondary bonds”. The interaction amounts to at least 15% – based on the overlap population data – of a “normal” I–I bond in  $I_3^-$ . This interpretation is also supported by the total electron density maps of  $I_2 \cdots I^-$  contacts at 5.0, 4.0 and 3.5 Å shown in Figure 6a–c. Below 4 Å there is a substantial electron density between the  $I_2$  and  $I^-$  fragments. The difference electron density map in Figure 7 gives more detailed information about the bonding scheme. When brought into contact with an  $I_2$  molecule (gradually from just above 4 Å), the  $I^-$  ion loses electron density from essentially a 5p orbital, and this electron density is transferred to the anti-

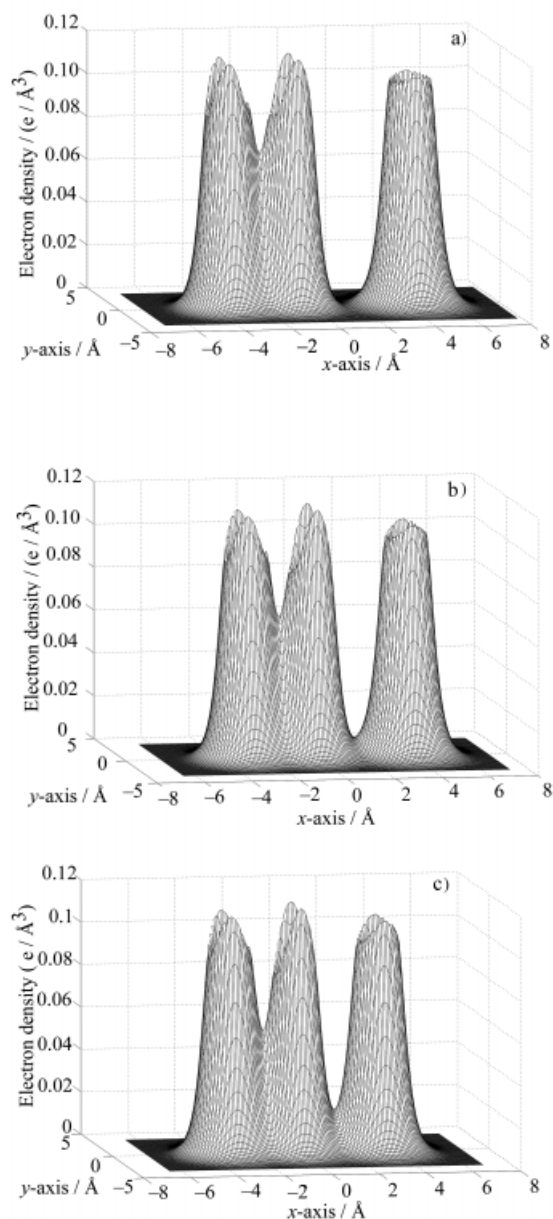


Figure 6. Total electron density of the  $I_2 \cdots I^-$  interaction in  $I_3^-$  at a) 5.0 Å, b) 4.0 Å and c) 3.5 Å

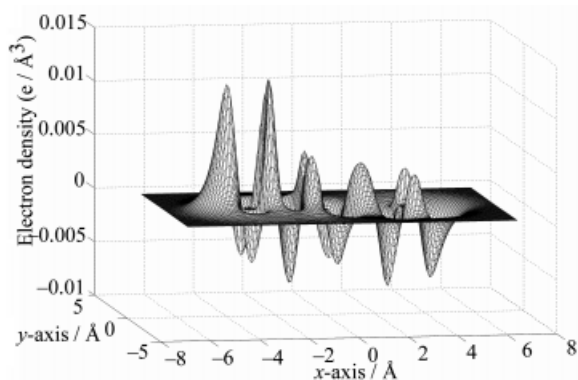
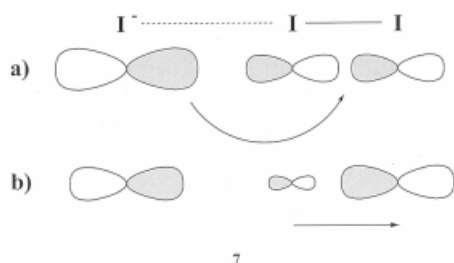


Figure 7. Difference electron density map of the  $\text{I}^- \cdots \text{I}_2$  interaction in  $\text{I}_3^-$  at 3.5 Å ( $\text{I}^-$  on the right-hand side)



bonding LUMO of 5p–5p character in the  $\text{I}_2$  fragment (a). As a secondary effect, the transferred electron density is polarized by the remaining negative charge on the  $\text{I}^-$  fragment (b), thus approaching the  $(-1/2)-(0)-(-1/2)$  charge distribution in the centrosymmetric  $\text{I}_3^-$  ion.

In order to further investigate the character of the bonding in  $\text{I}_3^-$ , the basis set superposition errors (BSSE) corrected interaction energy at the MP2 level was studied as a function of the distance between the centres of mass of the two fragments  $\text{I}_2$  and  $\text{I}^-$  up to 20 Å separation. The BSSE at 4 Å is estimated to account for 2% of the total interaction energy, which gives an indication of the corrections involved in the present analysis. At greater distances the interaction is dominated by ion–quadrupole interactions because of the strong quadrupole moment of  $\text{I}_2$  ( $-1.17 \cdot 10^{-38} \text{ Cm}^2$ ; MP2). The total interaction energy curve (IEC) is shown in Figure 8. The IEC is adequately described by ion–quadrupole, induction and dispersion interactions at distances greater than 7 Å. At shorter distances, the situation is of course complicated by the intramolecular interactions and charge-transfer effects. Here, a very simplistic approach is adopted: The long-range interactions are extrapolated down to the equilibrium I–I distance in  $\text{I}_3^-$  (about 3 Å). Although the induction and ion–quadrupole interactions were corrected for charges on the fragments, this is an oversimplification neglecting the damping of intermolecular interactions at shorter distances, especially concerning the dispersion interaction. Nevertheless, a maximum contribution to the total interaction energy in the “secondary bond” region may be estimated.

The remaining bonding interaction is assumed to arise mainly from intramolecular covalent and electrostatic interactions, which were modelled by a simple (exponential)

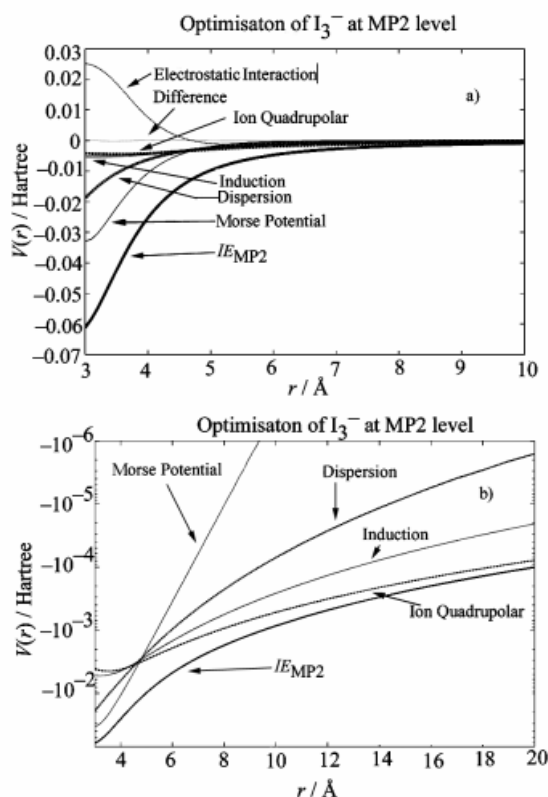


Figure 8. Interaction energy for the MP2 level and models as functions of the shortest distance between the fragments plotted in a) normal scale and b) logarithmic scale; the distance  $r$  refers to the distance between the centres of the iodide ion and the closest iodine atom in the  $\text{I}_2$  molecule

Morse potential. The overall fit is excellent. Several fundamental conclusions can be drawn from the results.

Firstly, based on the Morse potential obtained the covalent interaction is significant up to distances of at least 5 Å. In Figure 8 the electrostatic interaction based on the NBO charges of the  $\text{I}^-$  and  $\text{I}_2$  fragments is also included, although this was not used in the modelling of the total IEC. At greater distances the iodide ion induces a dipole on the iodine molecule, where polarization gives the closest iodine atom a partial positive charge and the most distant iodine atom a partial negative charge, resulting in a net attractive interaction. This situation prevails down to about 5 Å, where charge-transfer, inferring the beginning of orbital overlap, causes the repulsive factor to dominate. At shorter distances a strongly repulsive interaction is observed. The changeover from attractive to repulsive electrostatic interaction is at about 4.7 Å, thus giving an independent estimate of the extension of covalent interaction.

Secondly, in the region of “secondary bonds” (3–4 Å) the interaction energy is dominated by intramolecular and dispersion interactions. However, the dispersion contribution at these short distances is likely to be greatly overestimated. In addition, it is obvious from the repulsive electrostatic interaction that the covalent interaction compensates for extensive intramolecular ion–ion (or ion–dipole) repulsion. The results are very clear in one respect: There



is no specific justification based on bonding arguments for using a cut-off between intra- and intermolecular bonding somewhere in the region of “secondary bonds”.

We are of course aware of the classical controversy regarding the bonding description of the  $X_2-X_2$  interaction in condensed halogens, in particular that of  $Cl_2-Cl_2$  (see for instance ref.<sup>[9]</sup>). The extensive literature on this subject, in many cases reduced to semantics rather than chemistry, clearly shows that different bonding models can be used to rationalize the interhalogen bonding. It is not our intention to revive this controversy with the present work. There are obvious similarities and differences between the bonding situation in “pure” halogens and the polyiodides, where the higher charge-transfer capability of the ionic fragments in polyiodides is the most important difference. This is emphasized by adopting a frontier orbital view: the HOMO energy of  $I^-$  (the 5p orbitals) is  $-3.33$  eV, which should be compared with the HOMO ( $\pi_g$ ) and LUMO ( $\sigma_u$ ) energies of  $I_2$  at  $-9.78$  and  $-0.61$  eV, respectively; here all values are taken from the results of the MP2 calculations. For the interactions in the region from primary to “secondary bonds” between the ionic and neutral building blocks of the polyiodides, the collective data from correlation effects, bond-order calculations, intermolecular interaction modeling and electron-density distributions thus lead us to propose that the bonding between 3 and 4 Å is dominated by covalent interactions, with additional dispersion interactions. Recently, a similar approach was used by Boese and co-workers in the rationalization of the crystal structure of CIF.<sup>[10]</sup>

## The Pentaiodide System

The BSSE-corrected PES for a V-shaped  $I_5^-$  ion at the HF level is shown in Figure 9, corresponding to the configuration in **8** ( $r_2$  optimized for each  $\alpha$  and  $r_1$ ). As previously noted, the PES is very flat with respect to angular deformation. The optimum intermolecular ( $I^- \cdots I_2$ ) distances and angles ( $r_1/\alpha$ ) are  $3.267$  Å/ $110^\circ$  and  $3.048$  Å/ $102^\circ$  at HF and MP2 levels, respectively. This geometry and the structural data correspond well with those found experimentally. The difference PES at the MP2 level is shown in Figure 10. The

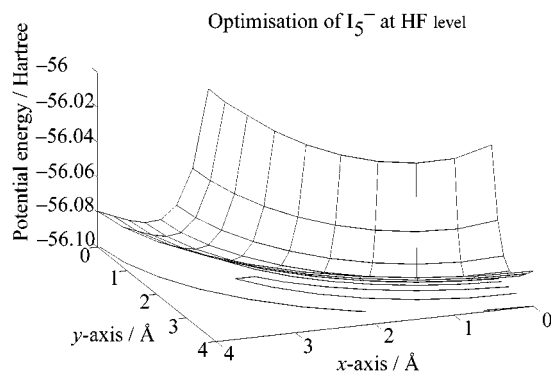


Figure 9. PES at the HF level for the V-shaped  $I_5^-$  ion ( $C_{2v}$  symmetry)

results of the theoretical study by Lin and Hall, where a decrease in intermolecular bond length is observed when dynamic correlation is taken into account, was taken as an indication of a substantial dispersion interaction.<sup>[11]</sup>

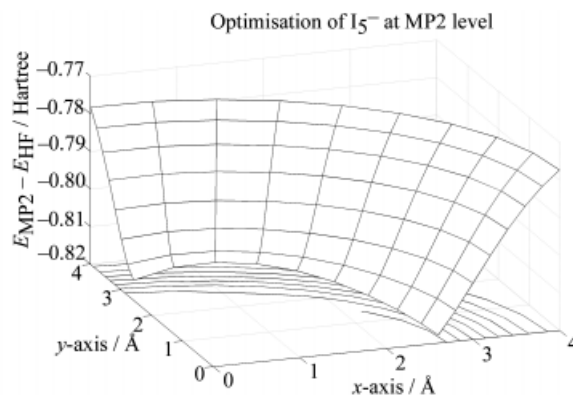
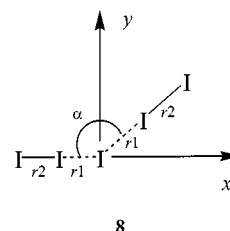


Figure 10. The difference PES between HF and MP2 levels for the V-shaped  $I_5^-$  ion



The same effect is seen in our results, where  $r_1$  decreases for the MP2 level calculation. However, the difference PES values are similar to those for the  $I_3^-$  ion in being less informative on the intermolecular stabilization caused by the dispersion interaction. Again, both the NLMO/NPA BOS in Figure 11 and the total electron density map of an  $I_5^-$  ion at the optimized parameters in Figure 12 instead indicate a substantial charge transfer or covalent interaction in the range of “secondary bonding”. Also, the difference electron density map shows a charge transfer from two independent 5p orbitals of the  $I^-$  fragment to the 5p–5p orbital-based LUMOs of the two  $I_2$  fragments, thus mimicking the bonding situation in  $I_3^-$  (Figure 13). The V-shaped  $I_5^-$  ion can essentially be visualized as consisting of two  $I_3$  legs with a common central iodine atom.

## Conclusions

The present structural, statistical and computational data give no justification for the postulation of a “secondary bond” region other than for purely pragmatic reasons with respect to structural description and rationalization. The chemical bonding in the “secondary bond” region (between 3 and 4 Å) can be very adequately described in terms of intramolecular bonding with an additional dispersion interaction between the  $I^-$  and  $I_2$  fragments in polyiodide compounds. The intramolecular interaction is comprised of attractive orbital overlap extending to almost 5 Å, compensating for a repulsive electrostatic interaction.

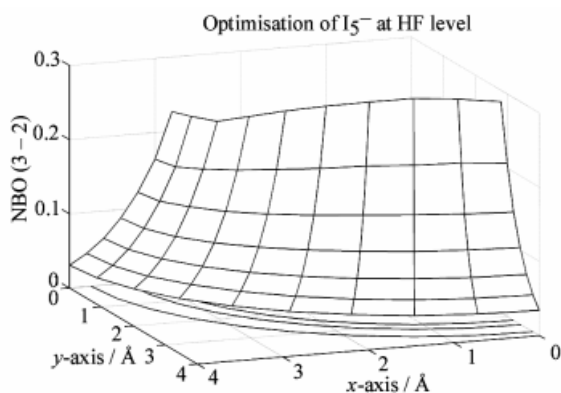


Figure 11. The NLMO/NPA BOS for the V-shaped  $I_5^-$  ion at HF level

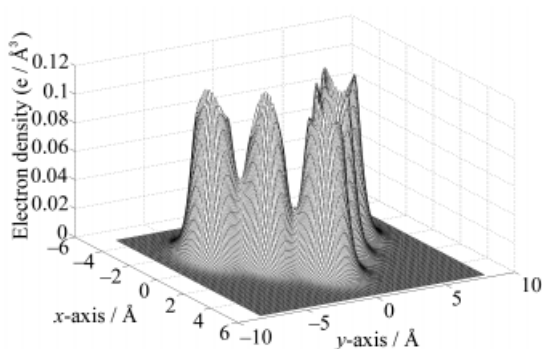


Figure 12. The total electron density of the  $I^- \cdots I_2$  interaction in  $I_5^-$

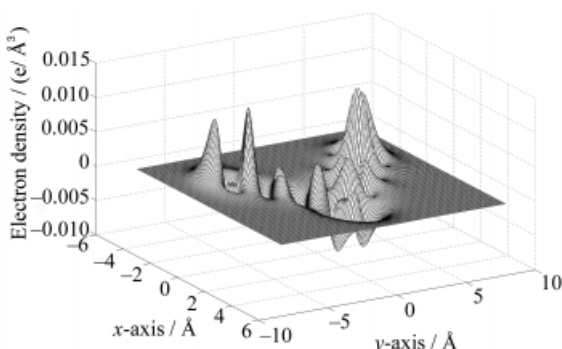


Figure 13. The difference electron density of the  $I^- \cdots I_2$  interaction in  $I_5^-$

## Databases and Computational Details

The structural statistical data were retrieved from the Cambridge Structural Database system (CSD).<sup>[12]</sup> Only structures with  $I \cdots I$  interactions within polyiodides were included (thus, for example,  $I \cdots I-S$  and  $I \cdots I-P$  interactions were excluded). Structures with disorder, errors and  $R \geq 10\%$  were excluded from the statistics. The database contains approximately 300 triiodides and 40 higher polyiodides. All quantum chemical calculations were performed us-

Table 1. Basis set for I (7s6p3d2f) optimized at the HF level

	Exponent
s	7.021141D+00
	6.344809D+00
	5.576563D+00
	1.437146D+00
	3.252227D-01
	1.568314D-01
p	7.549193D-02
	5.672424D+00
	3.655570D+00
	1.742992D+00
	3.736331D-01
	1.599806D-01
d	6.578836D-02
	1.325395D+00
	3.591044D-01
f	1.425310D-01
	5.212644D-01
	1.896558D-01

ing Gaussian 98 (revision A.7).<sup>[13]</sup> An ECP-based basis set was used for iodine, employing the Stuttgart group *quasi-relativistic* ECP and an uncontracted valence space (7s6p3d2f), see Table 1.<sup>[14]</sup> Calculations were performed at Hartree–Fock (HF), 2nd-order Møller–Plesset perturbation theory (MP2) and, where possible, coupled cluster levels including single and double excitations (CCSD). The PES values obtained were corrected for basis set superposition errors (BSSE). However, previous results for the  $I_3^- \cdots I_2$  and  $AuI_2^- \cdots I_2$  interactions suggest that the main features of these weak interactions are obtained without correction for BSSE.<sup>[15]</sup> In an attempt to describe the  $I^- \cdots I_2$  interaction, the interaction energy curve (IEC) at MP2 level out to 20 Å was determined, allowing the I–I distance of the iodine unit to relax at each step. The model interactions were fitted to the calculated IEC by least-squares methods. At greater distances the IEC was adequately described by ion–quadrupole ( $1/r^3$ ), induction ( $1/r^4$ ), and dispersion ( $1/r^6$ ) interactions.<sup>[16]</sup> The long-range interactions were fitted in the region 7–20 Å, while a Morse potential, used to model intramolecular interaction, was fitted in the region 3–20 Å. The induction and ion–quadrupole interactions were compensated for the charge on  $I^-$  by means of calculated NBO charges.

[1] P. H. Svensson, L. Kloo, *J. Chem. Soc., Dalton Trans.* **2000**, 2449.

[2] K.-F. Tebbe, R. Buchem, *Angew. Chem. Int. Ed. Engl.* **1997**, 36, 1345.

[3] P. H. Svensson, G. Raud, L. Kloo, *Eur. J. Inorg. Chem.* **2000**, 1275.

[4] M. Bittner, PhD Thesis, Universität zu Köln, **1994**.

[5] P. Pykkö, *Chem. Rev.* **1997**, 97, 597.

[6] A. D. Buckingham, P. W. Fowler, J. M. Hutson, *Chem. Rev.* **1988**, 88, 963.

[7] A. E. Reed, F. Weinhold, *J. Chem. Phys.* **1985**, 83, 1736; A. E. Reed, P. von Rague Schleyer, *J. Am. Chem. Phys.* **1990**, 112, 1434; E. D. Glénning, A. E. Reed, J. E. Carpenter, *Gaussian94 NBO*, version 3.1.

- [8] G. A. Landrum, N. Goldberg, R. Hoffmann, *J. Chem. Soc., Dalton Trans.* **1997**, 3605.
- [9] D. E. Williams, D. Gao, *Inorg. Chem.* **1997**, *36*, 782.
- [10] R. Boese, A. D. Boese, D. Bläser, M. Y. Antipin, A. Ellern, K. Seppelt, *Angew. Chem. Int. Ed. Engl.* **1997**, *36*, 1489.
- [11] Z. Lin, M. B. Hall, *Polyhedron* **1993**, *12*, 1499.
- [12] Cambridge Structural Database System, Database V. 5.22, **2001**.
- [13] M. J. Frisch, G. W. Trucks, H. B. Schlegel, G. E. Scuseria, M. A. Robb, J. R. Cheeseman, V. G. Zakrzewski, J. A. Montgomery, R. E. Stratmann, J. C. Burant, S. Dapprich, J. M. Millam, A. D. Daniels, K. N. Kudin, M. C. Strain, O. Farkas, J. Tomasi, V. Barone, M. Cossi, R. Cammi, B. Mennucci, C. Pomelli, C. Adamo, S. Clifford, J. Ochterski, G. A. Petersson, P. Y. Ayala, Q. Cui, K. Morokuma, D. K. Malick, A. D. Rabuck, K. Raghavachari, J. B. Foresman, J. Cioslowski, J. V. Ortiz, B. B. Stefanov, G. Liu, A. Liashenko, P. Piskorz, I. Komaromi, R. Gomperts, R. L. Martin, D. J. Fox, T. Keith, M. A. Al-Laham, C. Y. Peng, A. Nanayakkara, C. Gonzalez, M. Challacombe, P. M. W. Gill, B. G. Johnson, W. Chen, M. W. Wong, J. L. Andres, M. Head-Gordon, E. S. Replogle, J. A. Pople, *Gaussian* 98, Revision A.7, Gaussian, Inc., Pittsburgh, PA, **1998**.
- [14] A. Bergner, M. Dolg, W. Küchle, H. Stoll, H. Preuss, *Molec. Phys.* **1993**, *80*, 1431.
- [15] P. H. Svensson, J. Rosdahl, L. Klöö, *Chem. Eur. J.* **1999**, *5*, 305; J. Rosdahl, Diploma thesis, Lund University, **1997**.
- [16] A. J. Stone, *The Theory of Intermolecular Forces*, Clarendon Press, Oxford, **1996**.

Received November 6, 2000

[I00437]